Published in final edited form as:
Biochemistry. 2010 August 24; 49(33): 7033–7039. doi:10.1021/bi100749p.

Functional role of Thr-312 and Thr-315 in the proton-transfer pathway in *ba*$_3$ cytochrome *c* oxidase from *Thermus thermophilus*†

Irina Smirnova[1,2], **Joachim Reimann**[1], **Christoph von Ballmoos**[1], **Hsin-Yang Chang**[3], **Robert B. Gennis**[3], **James A. Fee**[4], **Peter Brzezinski**[1], and **Pia Ädelroth**[1,*]

[1]Department of Biochemistry and Biophysics, The Arrhenius Laboratories for Natural Sciences, Stockholm University, SE-106 91 Stockholm, Sweden

[3]Department of Biochemistry, University of Illinois, Urbana, IL 61801, USA

[4]Department of Molecular Biology, The Scripps Research Institute, La Jolla, CA 92037, USA

Abstract

Cytochrome *ba*$_3$ from *T. thermophilus* is a member of the B-type haem-copper oxidases, which have low sequence homology to the well-studied mitochondrial-like A-type. Recently, it was suggested that the *ba*$_3$ oxidase has only one pathway for proton delivery to the active site, and that this pathway is spatially analogous to the K-pathway in the A-type oxidases. This suggested pathway includes two threonines at positions 312 and 315. In this study, we investigated the time-resolved reaction between fully reduced cytochrome *ba*$_3$ and O_2 in variants where Thr-312 and Thr-315 were modified. While in the A-type oxidases this reaction is essentially unchanged in variants with the K-pathway modified, in the Thr-312→Ser variant in the *ba*$_3$ oxidase both reactions associated with proton uptake from solution, the P_R→F and F→O transitions, were slowed compared to the wild-type *ba*$_3$. The observed time constants were slowed ~3-fold (P_R→F, to ~170 μs from 60 μs in wild-type) and ~30-fold (F→O, to ~40 ms from 1.1 ms). In the Thr-315→Val variant, the F→O transition was about 5-fold slower (5 ms) than for the wild-type oxidase, whereas the P_R→F transition displayed an essentially unchanged time constant. However, proton uptake from solution was a factor of two slower and decoupled from the optical P_R→F transition. Our results thus show that proton uptake is significantly and specifically inhibited in the two variants, in strong support for the suggested involvement of the T312 and T315 in proton transfer to the active site during O_2 reduction in the *ba*$_3$ oxidase.

The *ba*$_3$ cytochrome *c* oxidase (C*c*O) from *Thermus (T.) thermophilus* is an integral membrane protein expressed at high temperatures and low oxygen concentrations. The *ba*$_3$ C*c*O is a member of the haem-copper oxidase (HCuO) superfamily, which are terminal oxidases that catalyse reduction of oxygen to water ($4\ e^- + 4\ H^+ + O_2 \rightarrow 2\ H_2O$) in a sequential mode, i.e. the reaction includes a number of reaction intermediates. The reaction is exergonic and a fraction of its free energy is conserved in the form of a transmembrane

†These studies were supported by grants from the Swedish Research Council (to P. B and P. Ä) and by the grant HL16101 from the National Institutes of Health (to R. B. G).

*Corresponding author: Telephone: +46-8-164183, Fax: +46-8-153679, piaa@dbb.su.se .
[2]Present address: A.N.Belozersky Institute of Physico-Chemical Biology, Moscow State University, Moscow 119899, Russia.

Supporting Information Available

Optical spectra of the WT, T312S and T315V *ba*3 variants. This material is available free of charge via the Internet at http://pubs.acs.org.

Unless otherwise noted, numbering of amino acid residues refer to subunit I in the *Thermus thermophilus ba*$_3$ oxidase.

electrochemical proton gradient. Energy conservation by terminal oxidases involves two different types of vectorial charge transfer: (i) a transfer of electrons and protons from opposite sides of the membrane (protons from the negative (in) N-side and electrons from the positive (out) P-side, respectively) to the catalytic site, where the oxygen chemistry occurs (Eq. 1a below), buried in the membrane and (ii) transfer of protons all across the membrane coupled to the redox reaction (proton pumping) (Eq. 1b). The observed proton pumping stoichiometry (*n* in Eq. 1b) varies between different members of the HCuO superfamily, in the ba_3 C*c*O ~0.5 H^+/e^- are pumped (1), compared to ~1 H^+/e^- for the aa_3-type oxidases.

$$O_2 + 4e^-_{out} + 4H^+_{in} \rightarrow 2H_2O \quad \text{(Eq. 1a)}$$

$$nH^+_{in} \rightarrow nH^+_{out} \quad \text{(Eq. 1b)}$$

According to the classification by Pereira *et al.*, ba_3 C*c*O belongs to the B-type oxidases displaying low sequence identity to HCuO members of type A, such as the aa_3 C*c*Os found in mitochondria, *Rhodobacter sphaeroides* or *Paracoccus denitrificans* (2). Like A-type HCuOs, the ba_3 C*c*O holds four redox-active sites, three of which are located in subunit I and include a low-spin haem *b* and a binuclear catalytic centre consisting of a high-spin haem a_{s3} (with the farnesyl side chain replaced by geranylgeranyl side chain (3)) and Cu_B. The fourth site is the di-nuclear Cu_A centre, located in subunit II, which acts as the primary electron acceptor from soluble cytochrome (cyt.) c^{552}. Amino acid residues, which serve as haem and Cu ligands, are conserved within the whole HCuO superfamily.

Like all other HCuOs, cyt. ba_3 requires specialized proton-conducting pathways for proton delivery from the N-side of the membrane through the hydrophobic barrier to the binuclear catalytic centre located approximately half-way through the membrane dielectric.

In a mitochondrial-like HCuO (the A1-type (2)) there are two proton-transfer pathways connecting the cytoplasmic compartment with the active site, called the D- and K-pathway, consisting of protonatable residues and water molecules (for a review on the general architecture of proton transfer pathways, see (4)). The D-pathway is used for both substrate (used in water formation) and pumped protons during the oxidative part of the catalytic cycle, whereas the K-pathway is used for proton uptake during the reductive part (see e.g. (5,6)). The D-pathway is named after an important aspartate (Asp-132, *R. sphaeroides* aa_3 numbering) located at the pathway entrance at the cytoplasmic surface, and the K-pathway is named after an essential lysine (Lys-362 in *R. sphaeroides* aa_3) in the middle of the pathway. The three-dimensional structure of ba_3 C*c*O from *T. thermophilus* was solved and originally three putative proton-conducting channels, leading from the cytoplasmic surface to the catalytic site, were proposed (3). One of them has a location in space equivalent to the K-pathway in A-type HCuOs. The other suggested proton pathway overlaps in part with the D-pathway in A-type HCuOs, and leads from the protein surface (Glu-17) to an internal cavity ~13 Å away from the catalytic site. Protons may be transferred to the catalytic site either directly from this cavity or via residues (Thr-81, Thr-394 and Ser-391) which are shared with the third suggested proton pathway called the Q-pathway. This putative pathway starts at a different surface Glu (Glu-254) and leads to the junction with the D-pathway.

The *T. thermophilus* ba_3 C*c*O has been cloned, enabling site-directed mutagenesis (7), which was used in a recent study in combination with sequence homology searches to suggest that B-type HCuOs use only one proton-conducting pathway (8). This pathway is the one equivalent to the K-pathway in the A-type oxidases, although made up from other amino

acids. The pathway (Figure 1) is built up mostly by residues in subunit I and leads to the conserved Tyr-237, which is covalently bound to the Cu_B ligand His-233. This pathway may start at the N-side of the membrane with Glu-516, Asp-517 and Ser-261 together with His-8(II) and Glu-15(II), where the two latter come from subunit II. Two of the residues of the K-pathway in *R. sphaeroides* aa_3 (Thr-359 and Lys-362) are replaced in ba_3 by Ser-309 and Thr-312. Other residues in the ba_3 pathway include Thr-315, Tyr-244, Tyr-248 and two structural water molecules.

The reaction of fully reduced ba_3 C*c*O with oxygen was recently independently studied with time-resolved approaches by two groups (9,10). The basic reaction sequence of the oxidative part of the catalytic cycle was shown to be similar to that of the aa_3-type oxidase (Figure 2). Initially, reduced haem a_{s3} binds oxygen with formation of the intermediate A (k ~1.7×10^8 $M^{-1}s^{-1}$) (9). Next, three electrons are taken from the binuclear center and one from the haem *b* in order to break the O-O-bond and an oxo-ferryl state (termed P_R) is formed at haem a_{s3} (k ~6.8×10^4 s^{-1}). In the next step, a proton is taken from the solution to the binuclear centre forming intermediate F and the electron on Cu_A re-equilibrates with haem *b* (k ~1.7×10^4 s^{-1}). Finally, the fully oxidized state is formed concomitantly with the uptake of the second proton from the solution (k ~1.1×10^3 s^{-1}).

In this study we investigated the reaction between fully reduced ba_3 and O_2 in ba_3 C*c*O variants where Thr-312 and Thr-315 in the suggested proton pathway were replaced by Ser and Val, respectively. These mutations slowed down enzyme turnover about 10-fold.

In the T312S variant, both transitions associated with proton uptake from solution, the $P_R\rightarrow F$ and $F\rightarrow O$ transitions, were slowed compared to the wild-type ba_3 C*c*O and occurred simultaneously with proton uptake from solution. Also in the T315V variant, the $F\rightarrow O$ transition was significantly slowed and coupled to proton uptake. However, the $P_R\rightarrow F$ transition occurred with an essentially unchanged rate constant, while proton uptake from solution was slowed by a factor of two, i.e. it followed in time after the $P_R\rightarrow F$ transition. The reductive part of the catalytic cycle in ba_3 C*c*O was investigated using the stopped-flow technique. Neither of these mutations had any effect on the reduction of haems *b* or a_{s3}.

In other words, our results show that proton uptake during the oxidative phase of the reaction is significantly and specifically inhibited in the two variants which supports the suggested involvement of the T312 and T315 in proton transfer to the active site.

Materials and methods

Bacterial growth and protein purification

Thermus thermophilus HB8 strain YC_1001 (bearing deletion of the *cba* gene and a plasmid with the ba_3 gene with a hepta-His-tag added at the N-terminal of the subunit I) was used as a source of wildtype (WT) and cytochrome ba_3 variants. Construction of the site-directed mutant ba_3 forms was described previously (7,8).

Cultivation of *Thermus thermophilus* HB8 and purification of the recombinant ba_3 C*c*O was performed essentially as described in (7). Small aliquots of concentrated solution of purified ba_3 C*c*O (60-80 μM) in 10 mM HEPES, pH 8.0, 0.05% dodecyl-β-D-maltoside (DDM) were kept at 4°C or flash-frozen in liquid nitrogen; in the latter case quick thawing was used in order to keep the enzyme intact. We observed no significant differences between the His-tagged WT ba_3 and the un-tagged enzyme studied previously (10).

Cytochrome c^{552} from *T. thermophilus* was purified as in (11).

Steady-state activity

Steady-state activity was monitored by recording oxygen consumption with Clark-type electrodes (Hansatech Oxytherm) at 23°C (295K). The starting solution contained 100 mM Hepes pH 7.5, 0.05% DDM, 6 mM ascorbate, 0.5 mM *N'*,*N'*,*N'*-tetramethyl-p-phenylenediamine (TMPD) and 5 μM cyt. c^{552}. The signal was allowed to stabilize before the reaction was started by the addition of 5 nM ba_3 C*c*O.

Sample preparation for flow-flash measurements

The cytochrome ba_3 samples were prepared as previously described (10). Briefly, samples containing cytochrome ba_3 in 100 mM HEPES-NaOH (pH 7.5), 0.05 % DDM and 5 μM phenazine methosulphate (PMS) were made anaerobic on a vacuum line, and air was exchanged for nitrogen. The enzyme was completely reduced (4 electrons/ba_3 C*c*O) by the addition of 2-3 mM sodium ascorbate and incubation from 1 h (at room temperature) to overnight (4°C). Then, nitrogen was exchanged for carbon monoxide and incubated for about 1-2 h at room temperature. Prolonged incubation was avoided due to a noticeable decrease in haem *b* absorbance (see Supporting Information).

Before transferring the fully reduced CO-bound ba_3 oxidase to the flow-flash syringe, CO recombination after flash photolysis was measured as a probe of the integrity of the binuclear site. The set-up for CO flash photolysis was described in (12).

Flow-flash experiments

Flow-flash experiments were performed using a locally modified stopped-flow apparatus (Applied Photophysics, DX-17MV) as described in (12). The enzyme solution was mixed with an oxygen-saturated solution (~1.2 mM oxygen) at a ratio of 1:5, and the reaction of the enzyme with oxygen was initiated by flash-photolysis (10 ns; 200 mJ; 532 nm, Nd-YAG laser from Quantel) of the enzyme-CO complex 30 ms after mixing. The short (30 ms) mixing time was used in order to minimise thermal dissociation of CO which has been shown to occur about 30-fold faster in ba_3 C*c*O than in aa_3-type HCuOs (13). Kinetics were monitored at different wavelengths (see Figures) and in two channels simultaneously so that traces were recorded on two different time-scales after the flash. The traces were fit to a sum of kinetic components.

Kinetics amplitudes were normalized to 1 μM reactive enzyme based on the CO-step at 445 nm using ε=67 mM^{-1} cm^{-1}.

Proton uptake measurements

Proton uptake during oxidation of the fully reduced enzyme by oxygen was measured as described (10). Briefly, the pH indicator dye cresol red (pK_a=8.3) was used since it has an absorbance maximum at 580 nm (deprotonated) where contribution of the haem *b* absorbance is significantly decreased. The sample buffer was exchanged for a buffer-free solution (100 mM KCl, 0.05% DDM, pH 8.0-8.2) using gel filtration on prepacked Sephadex G-25 column (PD-10; GE Healthcare). Traces were obtained also in the presence of buffer (100 mM Hepes, pH 8.0) and these traces were subtracted from those obtained in the buffer-free solution in order to exclude possible contributions from oxidation of the haems or reaction intermediates. In order to determine the amount of protons taken up during the oxidation of ba_3, the exhaust from the stopped-flow apparatus was collected and the ΔA^{580}/μM H^+ determined as described (10).

Measurement of the reduction rate of the haems

Reduction of the haems was monitored using a stopped-flow apparatus equipped with a diode array accessory (Applied Photophysics, SX-20 series). A solution of ~5 μM ba_3 in the oxidized form (as purified) in 100 mM HEPES-NaOH, pH 7.5, 0.1% Triton X-100, 0.05% DDM was mixed with an equal volume of the same buffer (without Triton X-100) and containing 30 mM dithionite as reductant and either 10 mM TMPD or 10 μM cyt. c^{552} as mediators. The diode array enabled us to monitor absorbance changes at multiple wavelengths simultaneously. For data evaluation, we subtracted a reference trace from the trace at the absorbance maximum of the individual haems in order to minimize artefacts from baseline drift or periodical noise. The reduction reactions of haems *b* and a_{s3} (see below for extinction coefficients) were monitored at 562.1 nm (with a reference wavelength at 575 nm) and at 611.4 nm (with a reference wavelength at 631.1 or 650.8 nm), respectively. About 7 traces were averaged. The rate constants were obtained by fitting the traces to a sum of kinetic components. The amount of haem reduced during the course of reaction was estimated from the reduced *minus* oxidized difference spectrum (see below) where the spectra obtained after 1 ms and ~5 minutes represent the oxidised and reduced species, respectively.

Determination of the haem concentrations

Haem *b* concentration was determined from a haem *b* reduced absolute spectrum with ε(560-590)= 26 $mM^{-1}cm^{-1}$ (7) or from a haem *b* reduced *minus* oxidized spectrum with ε(560-610)= 21 $mM^{-1}cm^{-1}$ (14). Ferro-haem a_{s3} was quantified using ε(613-658)= 6.3 $mM^{-1}cm^{-1}$ in the reduced minus oxidised spectrum. The CO-complex was quantified using ε(593-613)= 8.0 $mM^{-1}cm^{-1}$ from the CO-reduced *minus* reduced spectrum (14).

Results

Steady-state activity

Turnover numbers measured with ascorbate, cyt. c^{552} and TMPD (see Methods) at pH 7.5 in the different ba_3 variants were: wild-type: ~200 electrons/s, T312S: ~15 electrons/s and T315V: ~20 electrons/s. These values are in agreement with previously published data (8).

Optical spectra and CO recombination

A sample for a flow-flash experiment contains the reduced enzyme where haem a_{s3} is ligated with CO. Upon sample preparation (see M&M), we noted some spectral differences in the T312S and T315V ba_3 variants compared to WT (described in Supporting Information). These changes are, however, not expected to influence the interpretation of our kinetic data. CO recombination to the a_{s3} haem of the fully reduced ba_3 was studied as a probe of the integrity of the active site, and the observed rate constants were: wild-type: 5.1 s^{-1}, T312S: 4.6 s^{-1}, T315V: 3.5 s^{-1}, i.e. rate constants were approximately the same for the different forms of the ba_3 C*c*O.

Rapid absorbance changes during the reaction between fully reduced ba_3 variants and O_2

When the reduced CO-bound ba_3 is mixed with an oxygenated solution no reaction can proceed before CO is dissociated from the catalytic site. A short laser flash, applied shortly after mixing, releases CO and allows binding of O_2 and its sequential reduction to water. In the flow-flash apparatus, we detect the formation and decay of reaction intermediates using absorption spectroscopy.

We previously characterised the reaction between fully reduced wildtype ba_3 from *T. thermophilus* and O_2 ((10), see also (9)). Briefly, after the unresolved dissociation of CO

from haem a_{s3}, the first phase we observe is ascribed to P_R formation at k=6.8×10^4 s^{-1}, (τ~15 s).The second phase, with a rate constant of 1.7×10^4 s^{-1} (τ~60 s) is attributed to formation of the F* intermediate and re-reduction of haem *b*, concomitant with proton uptake from solution (see below).

Formation of F is followed by a (major) phase with a rate constant of 1100 s^{-1} (τ~0.9 ms), associated with transfer of the last electron from haem *b* and formation of the fully oxidized enzyme. Formation of O also has a small (less than 10% at all observed wavelengths) contribution from a phase with a rate constant of ~200 s^{-1} (τ~5 ms). Figure 3 shows the observed absorbance changes at 445 nm (reporting mainly on haem a_{s3}), 430 nm (mainly haem *b*), 560 nm (haem *b*) and 610 nm (haem a_{s3}).

The T312S and T315V variants displayed different kinetic characteristics from the WT C*c*O; the data are summarized in Table 1 and described below.

T312S—Formation of the P_R state was slowed down ~2-fold in T312S to ~3.3×10^4 s^{-1} (τ~30 μs, see Figure 3). The second phase, attributed to the P_R→F transition, was slowed more significantly (~3-fold) to k~6000 s^{-1} (τ~170 s), and coupled to proton uptake from solution (see below). The final step, formation of the oxidised enzyme was slowed ~30-fold and occurred at ~30 s^{-1} (τ~33 ms) in T312S#.

The absorbance maximum for reduced haem *b* in the α-region is at 560 nm. According to the obtained amplitude of the P_R→F transition in T312S, a smaller fraction of haem *b* was reduced during F formation (Figure 3C) in this variant compared to the WT C*c*O. The redox-state of haem *b* is monitored also at 430 nm, where the initial decrease in absorbance is dominated by oxidation of haem *b* during P_R formation. At this wavelength, the subsequent increase in absorbance associated with transient reduction of haem *b* during the P_R→F transition is less clearly seen in the T312S *ba*$_3$ variant than in the WT enzyme, consistent with a smaller fraction reduced haem *b*.

T315V—The rate constant for P_R formation was unchanged in the T315V mutant C*c*O, whereas the P_R→F transition (k~1.7×10^4 s^{-1} in WT) was slightly slowed to ~1.3×10^4 s^{-1}, and uncoupled from proton uptake from solution, which was about 1.5-fold slower (~8000 s^{-1}, see below). The final F→O transition occurred with a rate constant of ~200 s^{-1} (τ~5 ms).

Rapid proton uptake during oxidation of the fully reduced *ba*$_3$

Proton uptake associated with oxidation of the fully reduced *ba*$_3$ C*c*O was monitored with the pH-sensitive dye cresol red (Figure 4) at pH ~8.0 as in (10). The WT *ba*$_3$ C*c*O displays two major phases of proton uptake with rate constants of ~1.7×10^4 s^{-1} and ~1100 s^{-1} and approximately equal contributions, corresponding to formation of F and O intermediates, respectively. The net total proton uptake stoichiometry was ~1.5 H$^+$/*ba*$_3$.

In the T312S variant, two phases of proton uptake were observed with rate constants of ~6000 s^{-1} and ~25 s^{-1}, corresponding to the rate constants observed for the P_R→F and F→O transitions. The amplitude ratio of the fast phase (P_R→F) to the slow phase (F→O) was ~1:1. In the T315V variant, the first phase of proton uptake was observed with a rate constant of ~8500 s^{-1}, which was about 1.5-fold slower than the corresponding P_R→F

*Note that in the *ba*$_3$ C*c*O, formation of F is in itself not associated with any detectable absorbance change (9), as occurs in *aa*$_3$, where the peak shifts from 607 nm to 580 nm (15).

#In one T312S preparation, there was an additional phase that we have not assigned to any transition, with k~250s^{-1}, observed at 445 nm, contributing less than 20% to the total absorbance change.

transition (see Discussion below). The second phase had a rate constant of 200 s^{-1}, i.e. occurred concomitantly with the F→O transition. The amplitude ratio was ~1:1.

Both the T312S and T315V variants showed total proton uptake stoichiometry similar to the WT ba_3 C*c*O (Fig. 4).

Reduction of oxidised ba_3 variants

Reduction of ba_3 C*c*O was demonstrated to be much slower than oxidation (8) and could be studied using a stopped-flow apparatus. In this study, we used two systems of reductants: dithionite with either TMPD (as in (8)) or with cyt. c^{552} (the native reductant). The use of dithionite as the ultimate electron donor enabled mixing with an aerobic enzyme sample, since rapid scavenging of oxygen occurred during the mixing time of the instrument. The results showed that neither of the investigated mutations had significant impact on the reduction rates (Table 2).

Discussion

When the three-dimensional structure of ba_3 CcO from *T. thermophilus* was solved, ((3) see also (16)) three putative proton-conducting pathways (called D, Q, and K) were proposed (3). Sequence analysis in combination with site-directed mutagenesis indicated that only one of these pathways is functionally important for proton delivery (8), and it was suggested that the B-type oxidases use only one proton-delivery pathway for both substrate (used for water formation) and pumped protons. This is in contrast to the A-type HCuOs which use two different pathways (D and K) for proton transfer during different partial steps in the catalytic cycle; the D-pathway for protons (6-7) taken up during the oxidative phase (both chemical and pumped) and the K-pathway for protons (1-2) taken up during reduction (see e.g. (5,17)). In cytochrome ba_3, the suggested proton transfer pathway has a spatial location similar to that of the K-pathway in the aa_3-type oxidases although it is made up from different amino acid residues. The key residue of the K-pathway in *R. sphaeroides* aa_3 (Lys-362) is replaced in the ba_3 C*c*O by Thr-312. The Thr-315 sits slightly 'below' (towards the cytoplasmic side) Thr-312 in the pathway (see Fig. 1). Introduction of mutations T312S or T315V resulted in a decrease of the ba_3 turnover rate from ~200 e^-s^{-1} to 15-20 e^-s^{-1} ((8) and this study). Additionally, introduction of the valine at position 315 (but not the serine at position 312) deprived the ba_3 of proton-pumping activity (8).

Application of the flow-flash technique allowed us to pinpoint which (if any) partial steps of the oxidative half (reaction of the reduced cytochrome ba_3 with O_2) of the reaction cycle that were affected by these mutations. A sequential scheme of the reaction of the four-electron reduced cytochrome ba_3 with oxygen is shown in Figure 2. Two reaction steps involve proton uptake from the solution, the P_R→F and F→O transitions. Our results show that in both the T312S and T315V ba_3 variants, these transitions are slowed, which is in contrast to the situation in the aa_3-type C*c*Os, where alterations of residues in the K-pathway has no significant effect on these transitions (see e.g. (18)). Our results, discussed in more detail below, thus support the involvement of the T312 and T315 residues in proton delivery to the active site.

T312S

In T312S ba_3, the P_R→F transition rate constant decreased from ~1.7×10^4 s^{-1} (in WT) to ~6000 s^{-1}, a ~3-fold retardation. The rate constant for the F→O transition was slowed a factor of ~30, from ~1100 s^{-1} to ~30 s^{-1}.

Surprisingly, we observed a ~2-fold retardation (rate constant changed from ≈6.8×10^4 s^{-1} to ≈3.3×10^4 s^{-1}) also on the formation of the P_R state in T312S mutant while this step does not

involve any external proton neither in aa_3-type oxidases nor in cytochrome ba_3 ((10) and this study). However, in aa_3 C*c*O, the formation of P_R has been shown to involve internal proton transfer (19,20) from the active-site Tyr in order to break the O-O bond (21,22). Furthermore, in *R. sphaeroides* aa_3 C*c*O, formation of P_R was slowed in variants where residues in the K-pathway were modified, and it was suggested that the positively charged K-362 (which is spatially analogous to the T312 in ba_3) changes conformation during formation of P_R in order to charge-compensate for the additional negative charge in the active site (12). Although the Thr-312 in ba_3 can not be positively charged, the same principle of using alterations in the pathway to accommodate the change in charge at the active site might still apply and explain the small slowing of the formation of P_R in the T312S variant.

The 'central' role of the T312 in the pathway is also manifested in the substantial effects on the rates of proton transfer even though a change from threonine to a serine is relatively modest.

T315V

In the oxidative half of the catalytic cycle, the mutation T315V affected mostly the F→O transition where the rate constant was about 6-fold slower (~200 s^{-1}) than in the WT ba_3 (~1100 s^{-1}). The P_R→F transition occurred nearly as fast as in the WT enzyme (~1.3×10^4 s^{-1} compared to ~1.7×10^4 s^{-1}). However, proton uptake from solution was slower (k~8500 s^{-1}) than the optical transition, which is in contrast to the WT and T312S variants where these processes had the same rate constants. This observation can be explained by an internal proton transfer occurring with k~1.3×10^4 s^{-1}, enabling the P_R→F transition to take place although proton uptake from solution is indeed slowed. This scenario is similar to that in the D132N variant of the aa_3 C*c*O in *R. sphaeroides* (23), where proton uptake from solution is significantly slower than the P_R→F transition at the catalytic site. It should also be noted that in the model for the P_R→F transition in aa_3, the internal proton transfer is the rate-limiting step at k~$10^4 s^{-1}$, and proton uptake from solution occurs with k>>$10^4 s^{-1}$ (23). Translated to the scenario in the ba_3 oxidase, the observed retardation of proton uptake in the T315V mutant C*c*O to k~8500 s^{-1} is then due to slowed proton transfer from >>1.7×10^4 s^{-1} such that the actual retardation is much larger than the observed factor of ~2.

Since in T315V, the valine at position 315 is incapable of proton transfer, it can presumably be bypassed via a different residue indicating that the Thr-315 is not as central to the functioning of the pathway as Thr-312.

It should however be noted that the T315V mutation leads to a decoupling of the proton pump, in contrast to the T312S which retains pumping (8). Because in our flow-flash measurements, the observed transitions in the T312S ba_3 are more significantly slowed than in the T315V ba_3, this decoupling is not simply a result of slowing of proton uptake from the bulk solution. Instead it is likely that the decoupling is due to changes in the timing of internal proton transfers in the T315V mutant C*c*O, which would determine the pumping stoichiometry. In this mutant C*c*O proton uptake is decoupled from the optical P_R→F transition (which requires proton transfer to the catalytic site), which would lead to accumulation of an unprotonated form of an internal proton donor to the catalytic site.

We also note that in both the T312S and T315V variants, the F→O transition is more affected than the P_R→F transition, which is presumably linked to the observation that in ba_3 CcO, only the F→O transition (and not P_R→F) is linked to proton pumping across the membrane (9). This is in contrast to the situation in aa_3 C*c*O, where both the P_R→F and F→O transitions are linked to proton pumping (see e.g. (24)).

In the T312S and T315V ba_3 variants, the oxidative part of the catalytic cycle is affected, whereas the reductive part is largely unaffected (see table 2). This is in contrast to the situation in the T312V and E15A (in SU-II) ba_3 variants which were shown to be inhibited in both the oxidative and reductive parts of the reaction cycle (8). These mutations resulted in such significant retardation of the catalytic cycle that made it possible to use stopped-flow for studying also the oxidative phase. The observed retardation of both oxidative and reductive phases is different from the situation in aa_3-type oxidases, where mutations in the D-pathway affects mainly the oxidative phase, and mutations in the K-pathway affects mainly the reductive phase (see e.g. (5)). The retardation of both reduction and oxidation in the T312V and E15A ba_3 variants was thus seen as further evidence for the existence of only one proton pathway. However, even in the wildtype enzyme, the observed reduction rate of haem a_{s3} is slow (~10-15 s^{-1}, see Results and (8)). This is possibly due to the use of the 'as isolated' form of the ba_3 C*c*O, since the bovine C*c*O is known to reduce slower in the so-called 'resting' state than in the so-called 'pulsed' (recently oxidised, see (25) and references therein) form. It is thus possible that the serine at position 312 (T312S) or the bypass of the valine in the position 315 (T315V) are sufficient for the delivery of protons during these slower reactions of the reductive part of the cycle while they fail to fulfill this task during the fast reactions of the oxidative part. It is also possible that differences in the reduction rates between the wildtype and T312S and T315V variants would be observed under conditions where reduction of heme a_{s3} is faster.

In conclusion, in this study we have focussed on partial reaction steps during the catalytic cycle specifically linked to proton transfer, and our results show that altering the K-pathway residues T312 and T315 in ba_3 oxidase from *T. thermophilus* inhibits proton transfer during the oxidative phase, and support the identification of a proton pathway through the T312 and T315.

Supplementary Material

Refer to Web version on PubMed Central for supplementary material.

Acknowledgments

Ying Chen (The Scripps Institute) is acknowledged for assistance in the introduction of mutations and the preparation of mutant proteins.

Abbreviations

DDM	*n*-dodecyl-β-D-maltoside
F	ferryl-intermediate
k	the rate constant
PMS	phenazine methosulphate
P_R	peroxy-intermediate
TMPD	*N*,*N*,*N*',*N*'-tetramethyl-p-phenylenediamine
τ	time constant
WT	wildtype
C*c*O	cytochrome *c* oxidase
HCuO	haem-copper oxidase

References

(1). Kannt A, Soulimane T, Buse G, Becker A, Bamberg E, Michel H. Electrical current generation and proton pumping catalyzed by the ba3-type cytochrome c oxidase from Thermus thermophilus. FEBS Lett. 1998; 434:17–22. [PubMed: 9738443]

(2). Pereira MM, Santana M, Teixeira M. A novel scenario for the evolution of haem-copper oxygen reductases. Biochim. Biophys. Acta. 2001; 1505:185–208. [PubMed: 11334784]

(3). Soulimane T, Buse G, Bourenkov GP, Bartunik HD, Huber R, Than ME. Structure and mechanism of the aberrant ba(3)-cytochrome c oxidase from thermus thermophilus. Embo J. 2000; 19:1766–1776. [PubMed: 10775261]

(4). Wraight CA. Chance and design-Proton transfer in water, channels and bioenergetic proteins. Biochim. Biophys. Acta. 2006; 1757:886–912. [PubMed: 16934216]

(5). Brzezinski P, Ädelroth P. Pathways of proton transfer in cytochrome c oxidase. J. Bioenerg. Biomembr. 1998; 30:99–107. [PubMed: 9623811]

(6). Konstantinov AA, Siletsky S, Mitchell D, Kaulen A, Gennis RB. The roles of the two proton input channels in cytochrome c oxidase from Rhodobacter sphaeroides probed by the effects of site-directed mutations on time-resolved electrogenic intraprotein proton transfer. Proc. Natl. Acad. Sci. USA. 1997; 94:9085–9090. [PubMed: 9256439]

(7). Chen Y, Hunsicker-Wang L, Pacoma RL, Luna E, Fee JA. A homologous expression system for obtaining engineered cytochrome ba3 from Thermus thermophilus HB8. Protein Expr. Purif. 2005; 40:299–318. [PubMed: 15766872]

(8). Chang HY, Hemp J, Chen Y, Fee JA, Gennis RB. The cytochrome ba3 oxygen reductase from Thermus thermophilus uses a single input channel for proton delivery to the active site and for proton pumping. Proc. Natl. Acad. Sci. USA. 2009; 106:16169–16173. [PubMed: 19805275]

(9). Siletsky SA, Belevich I, Jasaitis A, Konstantinov AA, Wikström M, Soulimane T, Verkhovsky MI. Time-resolved single-turnover of ba3 oxidase from Thermus thermophilus. Biochim. Biophys. Acta. 2007; 1767:1383–1392. [PubMed: 17964277]

(10). Smirnova IA, Zaslavsky D, Fee JA, Gennis RB, Brzezinski P. Electron and proton transfer in the ba(3) oxidase from Thermus thermophilus. J. Bioenerg. Biomembr. 2008; 40:281–287. [PubMed: 18752061]

(11). Fee JA, Chen Y, Todaro TR, Bren KL, Patel KM, Hill MG, Gomez-Moran E, Loehr TM, Ai J, Thöny-Meyer L, Williams PA, Stura E, Sridhar V, McRee DE. Integrity of thermus thermophilus cytochrome c552 synthesized by Escherichia coli cells expressing the host-specific cytochrome c maturation genes, ccmABCDEFGH: biochemical, spectral, and structural characterization of the recombinant protein. Protein Sci. 2000; 9:2074–2084. [PubMed: 11152119]

(12). Brändén M, Sigurdson H, Namslauer A, Gennis RB, Ädelroth P, Brzezinski P. On the role of the K-proton transfer pathway in cytochrome c oxidase. Proc. Natl. Acad. Sci. USA. 2001; 98:5013–5018. [PubMed: 11296255]

(13). Giuffrè A, Forte E, Antonini G, D'Itri E, Brunori M, Soulimane T, Buse G. Kinetic properties of ba3 oxidase from Thermus thermophilus: effect of temperature. Biochemistry. 1999; 38:1057–1065. [PubMed: 9894002]

(14). Zimmermann BH, Nitsche CI, Fee JA, Rusnak F, Munck E. Properties of a copper-containing cytochrome ba3: a second terminal oxidase from the extreme thermophile Thermus thermophilus. Proc. Natl. Acad. Sci. USA. 1988; 85:5779–5783. [PubMed: 2842747]

(15). Morgan JE, Verkhovsky MI, Wikström M. Observation and assignment of peroxy and ferryl intermediates in the reduction of dioxygen to water by cytochrome c oxidase. Biochemistry. 1996; 35:12235–40. [PubMed: 8823156]

(16). Liu B, Chen Y, Doukov T, Soltis SM, Stout CD, Fee JA. Combined microspectrophotometric and crystallographic examination of chemically reduced and X-ray radiation-reduced forms of cytochrome ba3 oxidase from Thermus thermophilus: structure of the reduced form of the enzyme. Biochemistry. 2009; 48:820–6. [PubMed: 19140675]

(17). Wikström M, Jasaitis A, Backgren C, Puustinen A, Verkhovsky MI. The role of the D- and K-pathways of proton transfer in the function of the haem-copper oxidases. Biochim Biophys Acta. 2000; 1459:514–20. [PubMed: 11004470]

(18). Ädelroth P, Gennis RB, Brzezinski P. Role of the pathway through K(I-362) in proton transfer in cytochrome *c* oxidase from *R. sphaeroides*. Biochemistry. 1998; 37:2470–2476. [PubMed: 9485395]

(19). Hallén S, Nilsson T. Proton transfer during the reaction between fully reduced cytochrome c oxidase and dioxygen: pH and deuterium isotope effects. Biochemistry. 1992; 31:11853–9. [PubMed: 1332774]

(20). Karpefors M, Ädelroth P, Namslauer A, Zhen Y, Brzezinski P. Formation of the “peroxy” intermediate in cytochrome c oxidase is associated with internal proton/hydrogen transfer. Biochemistry. 2000; 39:14664–14669. [PubMed: 11087423]

(21). Proshlyakov DA, Pressler MA, Babcock GT. Dioxygen activation and bond cleavage by mixed-valence cytochrome c oxidase. Proc. Natl. Acad. Sci. USA. 1998; 95:8020–8025. [PubMed: 9653133]

(22). Gorbikova EA, Belevich I, Wikström M, Verkhovsky MI. The proton donor for O-O bond scission by cytochrome c oxidase. Proc. Natl. Acad. Sci. USA. 2008; 105:10733–10737. [PubMed: 18664577]

(23). Smirnova IA, Ädelroth P, Gennis RB, Brzezinski P. Aspartate-132 in cytochrome c oxidase from Rhodobacter sphaeroides is involved in a two-step proton transfer during oxo-ferryl formation. Biochemistry. 1999; 38:6826–6833. [PubMed: 10346904]

(24). Faxén K, Gilderson G, Ädelroth P, Brzezinski P. A mechanistic principle for proton pumping by cytochrome c oxidase. Nature. 2005; 437:286–289. [PubMed: 16148937]

(25). Verkhovsky MI, Morgan JE, Wikström M. Control of electron delivery to the oxygen reduction site of cytochrome c oxidase: a role for protons. Biochemistry. 1995; 34:7483–91. [PubMed: 7779792]

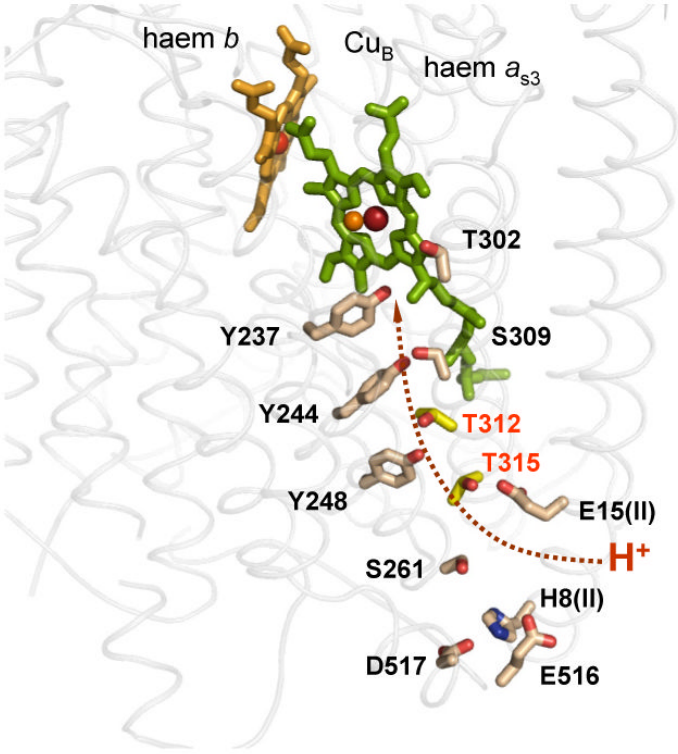

Figure 1.

Overview of the suggested proton-conducting K-pathway in ba_3 C*c*O from *T. thermophilus* (structure 1EHK) (3,8). Helices and loops are shown as a light-grey cartoon. Haem a_{s3} is shown in green; haem *b* is shown in light orange. Iron atoms of the haems and copper of Cu_B are shown in dark-red and orange, respectively. Side-chain atoms of the subunit I residues belonging to the proton-conducting pathway are shown in stick representation. The residues that were modified in this work are labeled in scarlet. Water molecules of the pathway are not shown.

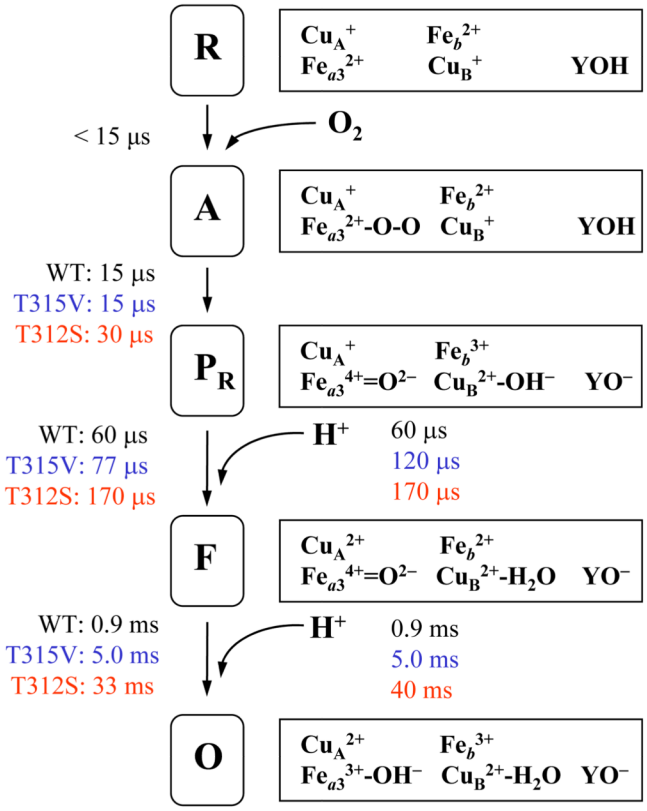

Figure 2.

A reaction scheme illustrating the oxidative part of the reaction cycle of the *ba*$_3$ C*c*O, modified from (10). The suggested structures of the intermediates are shown in rectangles to the right (Cu_A: copper A; Fe_b: the iron ion of haem *b*; Cu_B: copper B; Fe_{a3}: the iron ion of haem a_{s3} and Y: Tyr 237, the suggested proton-donor in the active site). Time constants for the optical transitions in WT and the T312S and T315V variants are shown to the left, an the rate constants for proton uptake to the right. Note that the R→A transition is not resolved in our measurements (but see (9)).

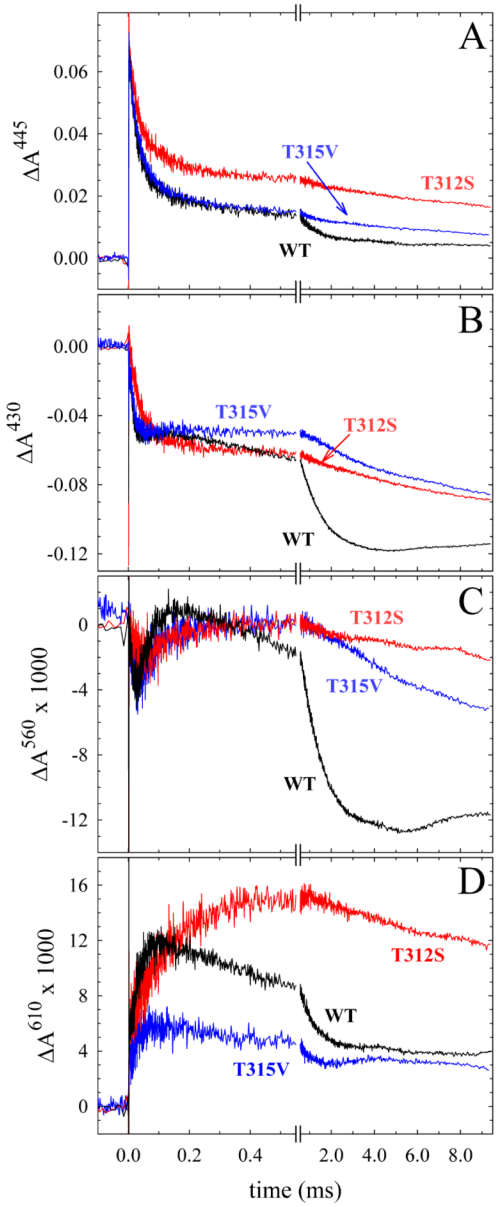

Figure 3.

Absorbance changes associated with reaction of the fully reduced ba_3 C*c*O with oxygen. Traces for WT, T312S and T315V are shown in black, red and blue, respectively. The absorbance changes were monitored at 445 nm (A), 430 nm (B), 560 nm (C) and 610 nm (D). Experimental conditions: 100 mM HEPES-KOH (pH 7.5); 0.05 % DDM; T=295K. Amplitudes are normalized to 1 μM reacting ba_3. The CO-ligand was dissociated by a laser flash at $t = 0$.

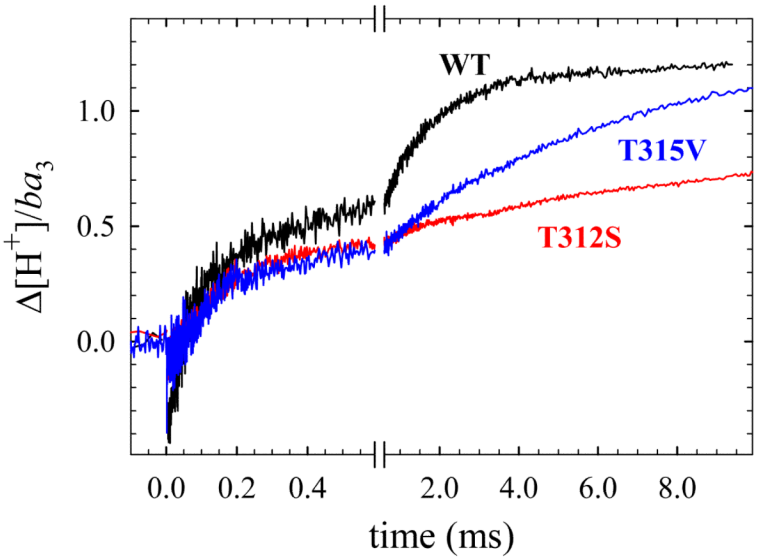

Figure 4.

Proton uptake upon reaction of the fully reduced WT, T312S and T315V ba_3 C*c*O with oxygen. Each trace is the difference between the averaged trace obtained without buffer and in the presence of buffer (see Materials and Methods). The trace for the WT enzyme is from (10). The amplitudes are normalized to 1 μM reacting enzyme. $\Delta H^+/ba_3$ determined as described in Materials and Methods. Experimental conditions: 100 mM KCl, 0.05% DDM, pH 8.0-8.2, 40 μM cresol red. Other conditions as in Fig. 3.

Table 1

Rate constants of the transitions observed in the flow-flash experiments

	Rate constant, s^{-1}		
	P_R formation	**P_R to F transition**	**F to O transition**
WT	6.8×10^4	1.7×10^4 *)	1.1×10^3
T312S	3.3×10^4	6.0×10^3 *)	30
T315V	6.8×10^4	1.3×10^4 **)	200

*) P_R to F transition was monitored indirectly via transient re-reduction of the haem *b* and proton uptake.

**) P_R to F transition was monitored via transient re-reduction of the haem *b*; proton uptake occurred at $k\sim8.5\times10^3$ s^{-1}.

Table 2

Reduction of the cytochrome ba_3 upon mixing with the reductants and mediators indicated. T=295K. For reaction conditions and details see *Materials and Methods*

***Ba*$_3$ variant**	**30 mM dithionite/10 mM TMPD, s^{-1}**		**30 mM dithionite/10 μM cyt. *c*^{552}, s^{-1}**	
	Haem *b*	**Haem a_{s3}**	**Haem *b***	**Haem a_{s3}**
WT	31	13	51	12
T312S	33	11	48	10
T315V	28	15	53	10